Chapter 1

Nuclear Fission I

> *"The discovery of fission, and its interpretation as a liquid-drop splitting, transformed nuclear physics from a laboratory science into a source of industrial power."*
>
> standard historical assessment [6, 14]

Nuclear fission is the splitting of a heavy nucleus into two fragments of comparable mass. Every commercial nuclear power reactor extracts energy from this process. In this chapter we define fission, recount the 1938–1939 discovery, derive the Q-value for symmetric fission from the semi-empirical mass formula (SEMF), obtain the energetic condition $Z^2/A > 17.6$, and explain why nuclei that are energetically free to fission still do not spontaneously split: the *fission barrier* of the Bohr–Wheeler liquid-drop picture. Neutron-induced fission and the compound-nucleus mechanism close the discussion and prepare the following lecture, *Nuclear Fission II*, [6, 1, 14, 2].

1.1 Definition and energy scale

Fission is the nuclear reaction in which a heavy parent X splits into two roughly equal fragments Y and Z,

$$X \;\rightarrow\; Y + Z \qquad (A \approx A_1 + A_2,\; Z \approx Z_1 + Z_2). \tag{1.1}$$

"Roughly equal" means the two fragments have comparable mass numbers; the extreme opposite is light-particle emission (α, proton, neutron), already treated in earlier chapters. In practice a few free neutrons are also emitted, so a more complete schematic is $X \rightarrow Y + Z + \nu n$ with $\nu \sim 2$–3. The essential physics is still the binary split of a heavy system into two medium-mass nuclei [6, 1].

Key idea

Fission: a heavy nucleus divides into two fragments of comparable mass ($A_1 \sim A_2$). Light-particle emission is *not* fission. Typical energy release for $A \sim 240$ is of order 200 MeV per event.

Why so much energy? The binding-energy-per-nucleon curve B/A versus A rises from light nuclei to a broad maximum near iron and nickel ($A \sim 56$–62, $B/A \sim 8.7$–8.8 MeV) and then *declines* slowly for heavy nuclei. For uranium-region nuclei ($A \sim 230$–240) one has $B/A \sim 7.6$ MeV; for fragments near $A \sim 100$–140 one finds $B/A \sim 8.5$ MeV. Moving nucleons from a low-B/A parent into higher-B/A daughters releases energy of order

$$Q \sim \left[(B/A)_{\text{frag}} - (B/A)_{\text{parent}}\right] A \sim (8.5 - 7.6)\,\text{MeV} \times 240 \approx 216\,\text{MeV}. \tag{1.2}$$

That is the characteristic fission energy scale. A full SEMF derivation of when $Q > 0$ occupies Section 1.4.

1.2 Historical path: neutrons, barium, and the liquid drop

Historical note

1932–1938: neutron irradiation and the search for transuranics. Chadwick's discovery of the neutron (1932) opened a new experimental tool: neutrons have no charge, so they are not repelled by the nuclear Coulomb field and can enter heavy nuclei even at thermal energies. Fermi's group in Rome systematically bombarded elements with neutrons, hoping that n capture followed by β^- decay would produce elements beyond uranium (transuranics). Many new radioactivities appeared; their chemical identification was difficult [6, 2].

1938–1939: Hahn and Strassmann. Otto Hahn and Fritz Strassmann irradiated natural uranium with neutrons and performed meticulous radiochemistry. Among the products they found an element that behaved chemically like barium ($Z = 56$), not like a heavy transuranic homologue of radium. After repeated checks they concluded that barium itself was present: a medium-mass element had been produced from uranium ($Z = 92$) [6, 14].

1939: Meitner, Frisch, and Bohr–Wheeler. Lise Meitner and Otto Frisch interpreted the result as a binary split of the uranium nucleus, by analogy with a charged liquid drop that divides when deformed. They estimated the energy release from the mass defect and named the process *fission*. Niels Bohr and John Wheeler then developed the liquid-drop theory of the fission barrier (1939), which still organises the subject [6, 1, 14].

The chemical surprise (barium from uranium) forced a change of paradigm: neutron irradiation of heavy nuclei does not only build slightly heavier species; it can also *break* the nucleus into two pieces of intermediate mass.

1.3 Binding energy and the Q-value of fission

Write the binary fission of a nucleus ${}^{A}_{Z}X_{N}$ as

$${}^{A}_{Z}X_{N} \;\to\; {}^{A_1}_{Z_1}Y_{N_1} + {}^{A_2}_{Z_2}Z_{N_2}, \tag{1.3}$$

with

$$A = A_1 + A_2, \qquad Z = Z_1 + Z_2, \qquad N = N_1 + N_2. \tag{1.4}$$

(We omit free neutrons for the mass-energy bookkeeping; they can be restored later without changing the logic.) Nuclear masses in energy units are

$$Mc^2 = Z\,m_p c^2 + N\,m_n c^2 - E_B, \tag{1.5}$$

where E_B is the total binding energy. The reaction Q-value is the decrease in rest mass,

$$Q = (M_X - M_Y - M_Z)c^2. \tag{1.6}$$

Substitute (1.5) for each nucleus. The proton and neutron mass terms cancel by charge and nucleon conservation, leaving

$$Q = E_B(Y) + E_B(Z) - E_B(X). \tag{1.7}$$

Fission releases energy if and only if the sum of the fragment binding energies exceeds the parent binding energy: the fragments are more tightly bound per nucleon (and overall) than the parent.

Numerical estimate from B/A. Take $E_B(X) = (B/A)_X\, A$ with $(B/A)_X \approx 7.6\,\text{MeV}$ and $E_B(Y) + E_B(Z) \approx 8.5\,\text{MeV} \times (A_1 + A_2) = 8.5\,\text{MeV} \times A$. Then

$$Q \approx (8.5 - 7.6)\,\text{MeV} \times A = 0.9\,\text{MeV} \times A. \tag{1.8}$$

For $A \approx 240$,

$$Q \approx 0.9 \times 240 = 216\,\text{MeV}, \tag{1.9}$$

as anticipated in (1.2). Systems tend toward lower rest-mass energy; fission of heavy nuclei is therefore energetically favoured once the fragments sit on the high-B/A side of the binding curve [6, 1, 2].

Remark

Equation (1.7) is general: any rearrangement of nucleons that increases total binding releases energy. Fusion of light nuclei, treated in later lectures, uses the same identity with the opposite motion on the B/A curve.

1.4 Symmetric fission from the SEMF: full derivation

To estimate when symmetric fission is energetically possible without external energy, use one nuclear-mass SEMF convention throughout this chapter, neglecting pairing and replacing $Z(Z-1)$ by Z^2:

$$M(A,Z)c^2 = Zm_pc^2 + Nm_nc^2 - a_vA + a_sA^{2/3} + a_c\frac{Z^2}{A^{1/3}} + a_{\text{sym}}\frac{(A-2Z)^2}{A}. \tag{1.10}$$

All a_i are energies. We use $a_s = 17.8\,\text{MeV}$ and $a_c = 0.711\,\text{MeV}$ in every numerical illustration; modest coefficient changes shift the thresholds because this is a liquid-drop estimate, not evaluated barrier data [6, 1, 14]. Consider *symmetric* fission into two identical fragments,

$$A_1 = A_2 = \frac{A}{2}, \qquad Z_1 = Z_2 = \frac{Z}{2}. \tag{1.11}$$

The Q-value in energy units is

$$Q = M(A,Z)c^2 - 2\,M\left(\frac{A}{2}, \frac{Z}{2}\right)c^2. \tag{1.12}$$

1.4.1 Term-by-term cancellation

Volume term.

$$-a_v A - 2\left(-a_v \frac{A}{2}\right) = -a_v A + a_v A = 0.$$

Volume energy is extensive; it cancels for any binary split that conserves A.

Asymmetry term. For the parent,

$$a_{\text{sym}} \frac{(A-2Z)^2}{A}.$$

For one fragment,

$$a_{\text{sym}} \frac{\big(A/2 - 2(Z/2)\big)^2}{A/2} = a_{\text{sym}} \frac{\big((A-2Z)/2\big)^2}{A/2} = a_{\text{sym}} \frac{(A-2Z)^2}{4} \cdot \frac{2}{A} = a_{\text{sym}} \frac{(A-2Z)^2}{2A}.$$

Two fragments contribute

$$2 \times a_{\text{sym}} \frac{(A-2Z)^2}{2A} = a_{\text{sym}} \frac{(A-2Z)^2}{A},$$

which exactly cancels the parent asymmetry term. Thus the symmetry energy drops out of Q for *symmetric* charge and mass partition.

Surface term.

$$Q_s = a_s A^{2/3} - 2\, a_s \left(\frac{A}{2}\right)^{2/3} = a_s A^{2/3} \left[1 - 2 \cdot \left(2^{-1}\right)^{2/3}\right] = a_s A^{2/3}(1 - 2^{1/3}).$$

Since $2^{1/3} \approx 1.260$,

$$Q_s = a_s A^{2/3}(1 - 1.260) = -0.260\, a_s\, A^{2/3}. \tag{1.13}$$

The surface term is *negative* in Q: two spheres have more total surface area than one sphere of equal volume, so surface energy opposes fission.

Coulomb term.

$$Q_c = a_c \frac{Z^2}{A^{1/3}} - 2\, a_c \frac{(Z/2)^2}{(A/2)^{1/3}} = a_c \frac{Z^2}{A^{1/3}} - 2\, a_c \frac{Z^2/4}{A^{1/3}\, 2^{-1/3}} = a_c \frac{Z^2}{A^{1/3}} - a_c \frac{Z^2}{2A^{1/3}}\, 2^{1/3}.$$

Using $2^{1/3}/2 = 2^{-2/3} \approx 0.630$,

$$Q_c = a_c \frac{Z^2}{A^{1/3}}(1 - 2^{-2/3}) = a_c \frac{Z^2}{A^{1/3}}(1 - 0.630) = 0.370\, a_c\, \frac{Z^2}{A^{1/3}}. \tag{1.14}$$

The Coulomb term is *positive* in Q: separating the charge into two smaller nuclei lowers the electrostatic self-energy and favours fission.

1.4.2 Net Q and the condition $Q > 0$

Collecting surface and Coulomb contributions,

$$\boxed{Q = -0.26\, a_s\, A^{2/3} + 0.37\, a_c\, \frac{Z^2}{A^{1/3}}} \tag{1.15}$$

(pairing neglected; volume and symmetry cancelled). Fission is energetically allowed when $Q > 0$; whether it occurs spontaneously is a separate barrier-penetration question:

$$0.37\, a_c\, \frac{Z^2}{A^{1/3}} > 0.26\, a_s\, A^{2/3}, \tag{1.16}$$

or equivalently

$$\frac{Z^2}{A} > \frac{0.26\, a_s}{0.37\, a_c}. \tag{1.17}$$

With the stated coefficients,

$$\frac{0.26 \times 17.8}{0.37 \times 0.711} \approx \frac{4.63}{0.263} \approx 17.6. \tag{1.18}$$

Hence the classic energetic criterion

$$\boxed{\frac{Z^2}{A} > 17.6 \quad \text{(symmetric fission energetically possible).}} \tag{1.19}$$

For nuclei along the valley of stability, $Z/A \sim 0.4$–0.45 at large A, so $Z^2/A \sim 0.16\, A$ to $0.20\, A$. The inequality $Z^2/A > 17.6$ is then satisfied for

$$A \gtrsim 100 \tag{1.20}$$

(roughly). All nuclei with $A \gtrsim 100$ are, on pure rest-mass grounds, candidates for spontaneous fission into two medium fragments [6, 1, 14, 2].

Key idea

Symmetric fission Q from SEMF: $Q = -0.26\, a_s A^{2/3} + 0.37\, a_c Z^2/A^{1/3}$. $Q > 0$ when $Z^2/A > 17.6$. Energetically, $A \gtrsim 100$ can fission. Volume and symmetry terms cancel; surface opposes, Coulomb drives fission.

Caution

Energetically allowed does *not* mean observed. Uranium and thorium have $A > 100$ and $Q > 0$, yet they are long-lived. The reason is the fission *barrier*: intermediate deformed shapes cost energy even when the final fragments lie lower than the parent (Section 1.5).

1.5 Why no spontaneous fission? The fission barrier

If $Q > 0$, why do ^{235}U and ^{238}U exist? The nucleus cannot jump discontinuously from a single sphere to two well-separated fragments. It must pass through a continuous sequence of deformed shapes at essentially constant volume (nuclear matter is nearly incompressible). Along that path the total energy $E(r)$ of the liquid drop first *rises*, then falls toward the asymptotic Coulomb repulsion of two fragments. The maximum of $E(r)$ relative to the ground-state energy is the **activation energy** or **fission barrier height** E_f [6, 1, 14].

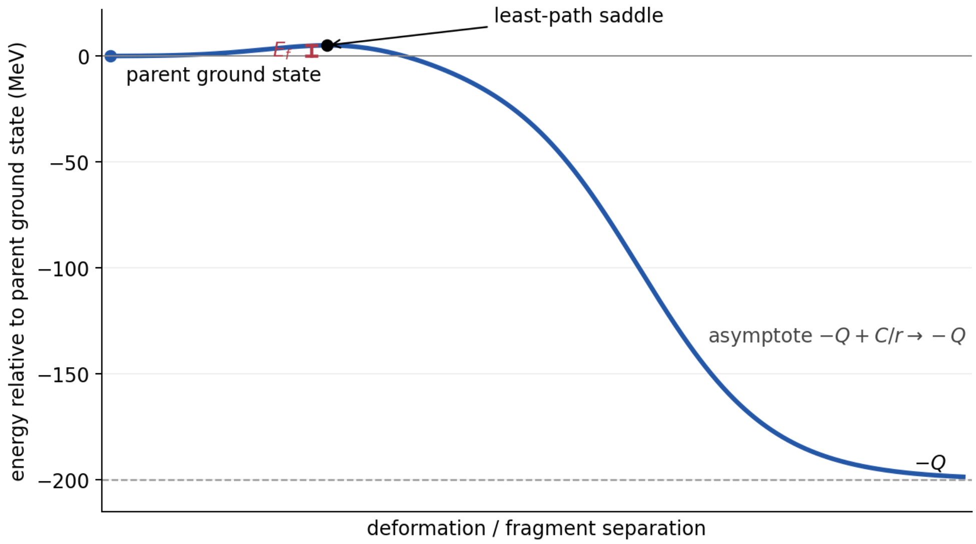

Figure 1.1: Schematic fission barrier, cleanly redrawn from the deformation-energy discussion in the original PH5001 Lecture 24 source: energy versus deformation (or fragment separation). The parent ground state sits in a well; a barrier of height E_f separates it from scission and the asymptote $-Q + C/r$. For $A \sim 240$, $E_f \sim 5.5$–6.5 MeV. The curve is schematic rather than evaluated data (Prof. Bharat Kumar, PH5001; compare H. C. Verma, NPTEL Lect. 33).

Physical competition. As the drop elongates:

- **Surface energy increases** (larger surface area at fixed volume).
- **Coulomb energy decreases** (protons move farther apart on average).

Near sphericity the surface penalty dominates for moderate Z^2/A, so $E(r)$ rises. On the parent-ground-state energy scale used in the figure, the large-separation asymptote is

$$E(r) \longrightarrow -Q + \frac{Z_1 Z_2 e^2}{4\pi\varepsilon_0 r}, \qquad r \to \infty. \tag{1.21}$$

The curve approaches $-Q$, not zero; the positive $1/r$ term is the remaining fragment repulsion. Between these limits a barrier peak appears (Fig. 1.1).

Energy reference. If the zero is chosen as two fragments at rest at infinite separation, the intact parent lies $Q \sim 200$ MeV *above* that zero. In the more usual deformation-energy plot one instead sets the parent ground state to zero; the separated products then lie at $-Q$, and the saddle lies at $+E_f$. These are the same curve shifted by a constant. Confusing the two zeros makes the roughly 200 MeV energy release look like the roughly 6 MeV activation barrier.

Barrier height for heavy nuclei. Bohr and Wheeler estimated E_f from the liquid-drop energy as a function of deformation. For uranium-region nuclei one finds typically

$$E_f \sim 5.5\text{–}6.5\,\mathrm{MeV}. \tag{1.22}$$

Spontaneous fission then requires either (i) thermal or quantum tunneling through a barrier of several MeV, which is extremely slow for $A \sim 240$, or (ii) supply of excitation energy comparable to E_f by a reaction (neutron capture, photon absorption, …). That is why uranium is metastable on geological timescales despite $Q > 0$ [6, 1].

1.6 Deformation energy: ellipsoid calculation

A quantitative sketch of the barrier near sphericity follows Bohr and Wheeler. Start with a spherical nucleus of radius R and deform it into a prolate ellipsoid of semi-axes a (long) and $b = b$ (equal short axes), at *constant volume*:

$$\frac{4}{3}\pi R^3 = \frac{4}{3}\pi a b^2 \quad \Rightarrow \quad R^3 = ab^2. \tag{1.23}$$

Parametrise a small elongation by

$$a = R(1+\varepsilon), \qquad b = \frac{R}{\sqrt{1+\varepsilon}} \tag{1.24}$$

(so that $ab^2 = R^3$ exactly). For small ε,

$$b = R\left(1 - \frac{\varepsilon}{2} + \frac{3\varepsilon^2}{8} + \mathcal{O}(\varepsilon^3)\right).$$

The square root and the factor 2 in the resulting fissility criterion are both lost in the OCR transcription of the original source.

For a prolate ellipsoid define $e^2 = 1 - b^2/a^2$. Its exact area is

$$S = 2\pi b^2 \left(1 + \frac{a}{be}\sin^{-1} e\right).$$

Using $e^2 = 3\varepsilon - 6\varepsilon^2 + \mathcal{O}(\varepsilon^3)$, $\sin^{-1} e/e = 1 + e^2/6 + 3e^4/40 + \cdots$, and the volume constraint gives

$$S \approx S_0\left(1 + \frac{2}{5}\varepsilon^2\right), \tag{1.25}$$

where $S_0 = 4\pi R^2$ is the sphere area. The surface energy therefore becomes

$$E_{\text{surf}} = a_s A^{2/3}\left(1 + \frac{2}{5}\varepsilon^2\right). \tag{1.26}$$

For a uniformly charged ellipsoid the shape dependence can be written

$$\frac{E_{\text{Coul}}}{E^{(0)}_{\text{Coul}}} = \frac{R}{2}\int_0^\infty \frac{\mathrm{d}s}{(b^2+s)\sqrt{a^2+s}}.$$

Expanding the integrand with the same a, b and evaluating the elementary integrals gives

$$E_{\text{Coul}} = a_c \frac{Z^2}{A^{1/3}} \left(1 - \frac{1}{5}\varepsilon^2\right). \tag{1.27}$$

(Surface grows; Coulomb falls as charge spreads along the long axis.)

The change in energy relative to the sphere is

$$\Delta E(\varepsilon) = E(\varepsilon) - E(0) = a_s A^{2/3} \cdot \frac{2}{5}\varepsilon^2 - a_c \frac{Z^2}{A^{1/3}} \cdot \frac{1}{5}\varepsilon^2 = \frac{\varepsilon^2}{5}\left[2a_s A^{2/3} - a_c \frac{Z^2}{A^{1/3}}\right]. \tag{1.28}$$

Here ΔE is the *increase in total liquid-drop energy* (equivalently the decrease in binding energy). This sign convention corrects a common OCR ambiguity in the source, where $B(\varepsilon) - B(0)$ and the deformation energy are interchanged. For the sphere to be *unstable* against infinitesimal deformation ($\Delta E < 0$ for any small $\varepsilon \neq 0$), one needs

$$2a_s A^{2/3} < a_c \frac{Z^2}{A^{1/3}}, \tag{1.29}$$

or

$$\frac{Z^2}{A} > \frac{2a_s}{a_c}. \tag{1.30}$$

With the chapter-wide coefficients,

$$\frac{2a_s}{a_c} \approx \frac{35.6}{0.711} \approx 50.1. \tag{1.31}$$

Thus

$$\frac{Z^2}{A} \gtrsim 50 \tag{1.32}$$

marks the loss of a barrier against small deformations: the nucleus is unstable at sphericity and fissions spontaneously with no activation energy. Taking $Z \approx 0.4A$ gives $Z^2/A \approx 0.16A$, so

$$A \gtrsim 300 \tag{1.33}$$

for barrierless spontaneous fission. No such nuclei exist as long-lived species; they would fission on nuclear timescales. Between the energetic threshold $Z^2/A \sim 18$ ($A \sim 100$) and the absolute instability $Z^2/A \sim 50$ ($A \sim 300$), nuclei are metastable: $Q > 0$ but $E_f > 0$ [6, 1, 14].

Remark

The ratio $x = (Z^2/A)/(Z^2/A)_{\text{crit}}$ is the classical *fissility* parameter. For uranium, $x \sim 0.7$–0.8: a finite barrier remains, but it is only a few MeV high.

1.6.1 Fissility and a Bohr–Wheeler barrier estimate

For a spherical liquid drop define

$$E_s^{(0)} = a_s A^{2/3}, \qquad E_C^{(0)} = a_c \frac{Z^2}{A^{1/3}}, \qquad x \equiv \frac{E_C^{(0)}}{2E_s^{(0)}} = \frac{a_c}{2a_s}\frac{Z^2}{A}. \tag{1.34}$$

Thus $x = 1$ is precisely the quadratic instability in Eq. (1.30). Keeping $Z(Z-1)$ rather than Z^2 gives the slightly more accurate classical expression but is immaterial for uranium. For ^{238}U, $Z^2/A = 35.56$; with $a_s = 17.8\,\mathrm{MeV}$, $a_c = 0.711\,\mathrm{MeV}$, one obtains $x \simeq 0.71$, so a finite barrier is expected.

The small-ε expansion proves local stability but cannot locate the saddle: a barrier height requires a family of shapes extending from a sphere to a necked drop. In the classical Bohr–Wheeler treatment one assumes

(i) an incompressible, uniformly charged drop with a sharp surface;

(ii) surface and direct Coulomb energies only (volume and symmetry terms are unchanged along a fixed-A, Z, constant-volume path);

(iii) axial, reflection-symmetric shapes and no shell, pairing, rotational, or dynamical corrections.

Writing the shape factors as

$$E_{\mathrm{def}}(\alpha) = E_s^{(0)}[B_s(\alpha) - 1] + E_C^{(0)}[B_C(\alpha) - 1], \qquad B_s(0) = B_C(0) = 1, \tag{1.35}$$

the physical liquid-drop barrier is the lowest saddle separating the initial minimum from scission:

$$E_f^{(\mathrm{LD})} = \min_{\mathcal{P}} \max_{\alpha\in\mathcal{P}} E_{\mathrm{def}}(\alpha), \tag{1.36}$$

where $\mathcal{P}$ runs over continuous deformation paths from the ground state to scission. The inner maximum finds the saddle crossed by one path; the outer minimum selects the least-energy path. Numerical minimisation over shape coordinates is the barrier calculation. There is no universal elementary closed form because the result depends on the shape family. A frequently quoted historical interpolation in the actinide region is

$$\boxed{E_f^{(\mathrm{LD})}(\mathrm{MeV}) \simeq 19.0 - 0.36\,\frac{Z^2}{A}} \tag{1.37}$$

and gives $E_f \simeq 19.0 - 0.36(35.56) = 6.2\,\mathrm{MeV}$ for ^{238}U. The constants 19.0 MeV and 0.36 MeV are fitted interpolation coefficients, not additional SEMF constants, so Eq. (1.37) must not be extrapolated to light nuclei or the superheavy region, nor presented as a universal Bohr–Wheeler derivation. Modern barriers are double-humped and include shell, pairing, equilibrium-deformation, and multidimensional-shape corrections. The robust Bohr–Wheeler result is the surface–Coulomb competition and $E_f \to 0$ as $x \to 1$, while the several-MeV value for a particular actinide is empirical/model-dependent [6, 14, 1].

1.7 Photofission and neutron-induced fission

1.7.1 Photofission

A γ ray deposits energy without changing A or Z:

$$\gamma + {}^{A}X \;\to\; \text{fission products.} \tag{1.38}$$

Photon absorption in heavy nuclei is strongest in the giant dipole resonance (GDR), where the proton and neutron fluids oscillate against one another. Absorption forms an excited nucleus with the original A, Z, but fission is only one decay branch:

$$\sigma_{\gamma f}(E_\gamma) = \sigma_{\rm abs}(E_\gamma)\frac{\Gamma_f}{\Gamma_f + \Gamma_n + \Gamma_\gamma + \cdots}.$$

Near threshold barrier penetration controls Γ_f; above particle threshold neutron emission can compete strongly, and the GDR line shape controls $\sigma_{\rm abs}$. Consequently photofission need not rise monotonically or "saturate" above E_f. It probes both the barrier and channel competition [6, 1].

1.7.2 Neutron-induced fission and the compound nucleus

A neutron can induce fission by forming a compound nucleus that is already excited:

$$n + {}^{A}X \ \rightarrow \ {}^{A+1}X^* \ \rightarrow \ \text{fission products}. \tag{1.39}$$

The excitation energy of the compound system is essentially the capture Q-value plus the kinetic energy of the neutron (centre-of-mass corrections are small for heavy targets). If that excitation exceeds E_f, fission is likely; if not, the system must tunnel, and the fission cross section remains tiny. Competing channels include elastic scattering and radiative capture (n, γ).

Whether thermal neutrons suffice depends on the capture Q-value relative to the barrier of the compound nucleus. That comparison for ^{235}U versus ^{238}U is the central theme of the next chapter [6, 1, 2].

Takeaway

- Fission: heavy $X \to Y + Z$ with $A_Y \sim A_Z$; $Q \sim 200\,\text{MeV}$ for $A \sim 240$ from the rise in B/A.
- History: neutron discovery (1932); Hahn–Strassmann barium (1939); Meitner–Frisch interpretation; Bohr–Wheeler barrier theory.
- SEMF symmetric $Q = -0.26 a_s A^{2/3} + 0.37 a_c Z^2/A^{1/3}$; $Q > 0$ for $Z^2/A > 17.6$ ($A \gtrsim 100$).
- Barrier from surface vs Coulomb along the least-energy deformation path; $E_f \sim 6\,\text{MeV}$ for $A \sim 240$; no barrier for $Z^2/A \gtrsim 50$ in the stated SEMF convention.
- Induced fission: photofission reflects GDR absorption, barrier penetration, and decay competition; neutron capture forms B^* with excitation $\approx Q_{\rm capture} + K_n$.

1.8 Deeper physics: fissility Z^2/A and the Bohr–Wheeler barrier

1.8.1 The fissility parameter

Liquid-drop fission balances Coulomb repulsion against surface tension. The dimensionless **fissility parameter**

$$\frac{Z^2}{A} \tag{1.40}$$

measures how strongly Coulomb destabilises a nucleus relative to its size [6, 14]. Empirically, spontaneous fission half-lives shorten rapidly once Z^2/A exceeds a critical value of order 45–47 [6, 1]. Light nuclei have small Z^2/A and are stable against fission; very heavy nuclei with large Z and moderate A sit in the fissile region where α decay, spontaneous fission, and cluster emission compete (Lectures 16–17).

Fissility of actinides and lead

For ^{235}U: $Z^2/A = 92^2/235 \approx 36.0$. For ^{238}U: $92^2/238 \approx 35.6$. For ^{208}Pb: $82^2/208 \approx 32.3$ [6]. Both uranium isotopes are fissionable with induced neutrons; ^{208}Pb lies well below the spontaneous-fission threshold. The small difference in Z^2/A between ^{235}U and ^{238}U combines with pairing effects to explain why thermal-neutron fission of ^{235}U dominates reactor physics (Lecture 24) [1, 35].

1.8.2 Bohr–Wheeler barrier estimate

In the Bohr–Wheeler picture, fission proceeds by deforming the nucleus from a sphere of radius $R = r_0 A^{1/3}$ into two touching spheres. The Coulomb energy rises and the surface energy falls; the barrier height is set by the competition. A schematic result is

$$B_f \approx a_S A^{2/3} \left(1 - \frac{Z^2/A}{a_S/a_C}\right)^2, \tag{1.41}$$

with surface and Coulomb coefficients a_S and a_C from the SEMF [6, 14]. When Z^2/A approaches the critical value, $B_f \to 0$ and fission becomes instantaneous on nuclear time scales. Shell corrections modify this picture: double-humped barriers and asymmetric yields require microscopic potential-energy surfaces (Lecture 24) [6, 54].

Key idea

Same tunneling language as α decay. Spontaneous fission can be viewed as tunneling through a multidimensional barrier, the heavy-nucleus analogue of the Gamow integral (Lecture 17). A 1 MeV uncertainty in barrier height can change the half-life by orders of magnitude, which is why modern fission theory emphasises collective inertia and dissipation alongside B_f [54, 6].

1.8.3 Induced fission and the compound nucleus

Neutron-induced fission proceeds through a compound nucleus $X + a \to C^* \to f_1 + f_2 + n + \cdots$ with $Q > 0$ for fissile targets [6, 1]. The saddle barrier B_f is an extra energy requirement beyond the Q-value: fast neutrons supply enough excitation to overcome B_f in ^{238}U, breeding ^{239}Pu after β^- decay (Lecture 24) [35]. The liquid-drop fissility Z^2/A explains why actinides fission while lead does not, but asymmetric yields require shell corrections beyond (1.41) [14, 54].

1.8.4 Double-humped barriers and shape isomers

For actinides the fission potential-energy surface often shows two barriers with a secondary minimum (shape isomer) at large deformation [6, 14]. Delayed fission and intermediate structure in fission cross sections are experimental signatures. The simple single-barrier sketch of the main lecture is the first approximation; microscopic calculations on multidimensional surfaces reproduce the double-humped structure and the asymmetric valleys that drive mass yields (Lecture 24) [54]. Spontaneous-fission half-life systematics correlate with Z^2/A but show large odd–even staggering from pairing [6, 20].

Shell-corrected barriers explain why some actinides are metastable against fission despite large Z^2/A. Odd nucleons often hinder spontaneous fission relative to even–even neighbours. Those systematics matter for SHE survival probabilities (Lecture 25) and for astrophysical fission cycling (Lecture 24).

1.9 Further physics from the literature

Asymmetric fission and shell corrections. The pure liquid drop predicts a preference for *symmetric* mass splits near the barrier, yet thermal-neutron fission of ^{235}U is strongly asymmetric (peaks near $A \sim 95$ and $A \sim 140$). Strutinsky shell corrections to the liquid-drop energy create secondary minima and drive the mass-asymmetric valleys observed experimentally. The following fission lecture returns to yield curves; the microscopic theory is developed in advanced texts [6, 14, 2].

Spontaneous fission half-lives. Even with $Q > 0$, spontaneous fission half-lives range from milliseconds (very heavy Z) to 10^{15} years and beyond. Systematics correlate roughly with Z^2/A: larger fissility, lower barrier, shorter half-life. Pairing and shell structure produce large odd–even staggering [6, 1, 20].

Double-humped barriers. For actinides the potential energy surface often shows two barriers with a secondary minimum (shape isomer). Delayed fission and intermediate structure in fission cross sections are experimental signatures. The simple single-barrier sketch of Fig. 1.1 is the first approximation [6, 14].

Historical reading. Meitner and Frisch's 1939 note and Bohr and Wheeler's physical review article remain readable introductions. Modern textbook accounts that follow the same SEMF algebra as this chapter include Krane Ch. 13, Dunlap's fission chapter, and Basdevant *et al.* [6, 1, 14].

Open lecture sequence and data checks. H. C. Verma's IIT Kanpur/NPTEL course *Nuclear Physics: Fundamentals and Applications* places "Nuclear Fission Basics," "Nuclear Fission of Uranium," and "Nuclear Fission Reactor" consecutively as Lectures 33–35 (course 115104043). That sequence motivates the present division: energetics and deformation first, uranium and chain kinetics second. Numerical masses and separation energies should be checked against NNDC QCalc (AME2020); fission yields and neutron multiplicities should be checked against IAEA/NDS or ENDF rather than inferred from the liquid-drop model [32, 27, 35, 33].

Reading guide

Krane [6] Ch. 13 (energetics and barrier); Dunlap [1] (liquid drop and Q); Basdevant [14] (fissility and deformation); Demtröder [2] (historical and experimental overview). Evaluated fission data: ENSDF and NuDat 3 [20, 21].

1.9.1 Microscopic correction to the fissility estimate

The liquid-drop fissility parameter (1.40) captures the average trend of spontaneous-fission half-lives but misses shell structure. Strutinsky corrections add oscillatory terms to the potential-energy surface, creating double-humped barriers and asymmetric fission valleys [6, 54]. For ^{235}U, shell-stabilised fragments near $A \approx 95$ and 140 lower the asymmetric saddle relative to symmetric split, reversing the naive liquid-drop preference (Lecture 24) [14, 1].

WKB sensitivity of spontaneous-fission lifetime

Suppose a one-dimensional fission barrier has height $B_f = 6\,\text{MeV}$ and curvature radius $\hbar\omega \approx 1\,\text{MeV}$. A WKB estimate gives $\log_{10} t_{1/2} \propto B_f/\hbar\omega$. Raising B_f by 1 MeV can increase $t_{1/2}$ by ten to twenty orders of magnitude [6, 54]. This exponential sensitivity mirrors the Gamow factor in α decay (Lecture 17) and explains why microscopic barrier heights must be known to keV precision for quantitative half-life predictions.

1.9.2 From fission barriers to fusion and α competition

Very heavy nuclei sit in a competition zone: α decay (small Q_α lengthens lifetimes), spontaneous fission (large Z^2/A shortens them), and cluster emission (rare) [53, 6]. Superheavy synthesis chains terminate when both α and fission channels have short half-lives. Fusion-evaporation reactions (Lecture 25) populate the same Z, N region from the opposite direction: capture followed by neutron evaporation competes with quasifission [53, 52]. The Bohr–Wheeler picture is the macroscopic backbone; microscopic inertias set the dynamical timescale at scission.

Remark

Induced fission cross sections rise sharply once $E_{\text{CM}} > B_f$, analogous to sub-barrier fusion rising once tunneling through V_{max} becomes appreciable. Both are barrier-penetration phenomena, but fission involves a multidimensional saddle while fusion uses a one-dimensional entrance channel [54, 14].

1.9.3 Spontaneous fission versus α chains in superheavy nuclei

For $Z > 110$, spontaneous fission half-lives can fall below α-decay half-lives even when Q_α is favourable [53, 6]. SHE synthesis chains therefore terminate when neither channel allows further Z increase. The same Z^2/A diagnostic that classifies ^{235}U as fissionable predicts the onset of millisecond spontaneous fission in transfermium isotopes. Fusion evaporation (Lecture 25) and α emission (Lecture 16) are the two dominant de-excitation paths of the hot compound nucleus that sits above the fission saddle [53, 52].

1.9.4 Fragment kinetic energy and shell stabilisation

Total kinetic energy distributions in fission reflect Coulomb repulsion at scission and shell stabilisation of fragments [54, 6]. Models that agree on barrier height B_f can still disagree on kinetic energy and neutron multiplicity because scission dynamics and dissipation differ [54]. Asymmetric mass yields (Lecture 24) correlate with high kinetic energy in the heavy fragment peak near $A \approx 140$. The fissility parameter Z^2/A is therefore only the first diagnostic: fragment observables test dynamics beyond the static liquid-drop barrier [14, 1].

1.10 Deeper reading: Z^2/A, barriers, and microscopic dynamics

Bohr–Wheeler fissility compares Coulomb to surface energy. The dimensionless combination Z^2/A organises which nuclei have barriers against fission. Modern theory replaces a one-dimensional barrier with multidimensional potential-energy surfaces and collective inertias; half-lives remain exponentially sensitive to barrier height (Lecture 17).

Spontaneous fission of superheavy elements and fission recycling in the r-process both inherit this sensitivity. Evaluate Z^2/A for ^{235}U, ^{238}U, and ^{208}Pb as a standard exercise before reading yield distributions in Lecture 24.

Barrier systematics

Barrier heights decrease as Z^2/A increases, with shell corrections producing local islands of stability against fission. Odd-particle hindrance can add orders of magnitude to spontaneous-fission half-lives. Those systematics feed SHE survival estimates (Lecture 25).

Dissipation and scission

Post-barrier dynamics (friction, neck rupture) shape total kinetic energies and neutron multiplicities even when the static barrier is fixed. Models agreeing on B_f may still disagree on yields (Lecture 24). Ask which observables a microscopic fission paper was tuned to reproduce.

Fissility map

Compute Z^2/A for ^{232}Th, ^{235}U, ^{238}U, ^{246}Cm, and ^{208}Pb. Order them and discuss which have low fission barriers. Then sketch a one-dimensional barrier of height $B_f = 6\,\text{MeV}$ versus $5\,\text{MeV}$ and argue why thermal-neutron fission of ^{235}U is special once pairing and the barrier of the compound nucleus are considered (preview of Lecture 24).

Read a modern fission-theory abstract and list whether it constrains barriers, yields, kinetic energies, or half-lives. Different observables stress different parts of the multidimensional dynamics. Lecture 17's WKB lesson explains the half-life sensitivity; this chapter explains why the barrier itself depends on Z^2/A and shells.

Fissility organises barriers; microscopic dynamics organise yields and kinetic energies. Exponential lifetime sensitivity ties this chapter to Lecture 17.

In practice, rework one numerical estimate from the lecture with a different parameter set and compare the shift to the quoted experimental uncertainty. If the shift exceeds the uncertainty, the estimate is teaching a scale, not delivering a fit. That distinction keeps theoretical cartoons honest when they sit beside evaluated data tables and modern many-body calculations. Along the course arc, write one sentence linking this chapter backward and one forward: the discipline of those two sentences is as important as any single formula. Examination problems rarely ask for a literature review, but they do ask for the scale argument that literature reviews presuppose.

Synthesis problem

Write a half-page note that (i) restates the chapter's central scale or selection rule in one equation, (ii) evaluates it numerically for one concrete nucleus or energy, and (iii) names the neighbouring lecture that uses the result. Keep the note free of research-frontier speculation; the goal is fluency with the lecture physics itself. If an assumption fails (Born approximation, spherical mean field, allowed transition, one-dimensional barrier), state the failure mode in a final sentence. That habit converts passive reading into examination-ready understanding and makes the later research-frontier box read as an extension rather than a replacement.

Research frontier: microscopic fission dynamics and student projects

Bohr–Wheeler fissility (Lecture 23) explains the qualitative onset of fission through the competition of Coulomb and surface energies. Modern theory computes multidimensional potential-energy surfaces, collective inertias, and dissipative dynamics to predict barriers, half-lives, and fragment yields [54]. The same microscopic tools inform spontaneous fission of superheavy nuclei and fission recycling in the r-process [53, 52]. Remaining uncertainties in barrier heights of even 1 MeV can change half-lives by orders of magnitude; fragment-yield distributions for exotic actinides are still only partially constrained by experiment. Dissipation and scission dynamics remain active theory topics because different models can agree on barriers yet disagree on kinetic-energy and neutron-multiplicity observables. The lecture's fissility parameter Z^2/A remains the correct first diagnostic before those microscopic complications are introduced.

Yield and total kinetic energy distributions encode dynamics beyond the static barrier: shell-stabilised fragments, energy dissipation, and the timing of neck rupture. Microscopic models that agree on B_f can still disagree on those observables, which is why fission theory is not finished once a fissility formula is written down.

Models that match barriers but miss total kinetic energies are incomplete; dynamics beyond fissility remain part of the research frontier.

Student reviews should therefore ask which observables each microscopic model was tuned to reproduce.

Student directions. (1) Fissility exercise: evaluate Z^2/A for ^{235}U, ^{238}U, and ^{208}Pb and discuss the trend. (2) WKB insight: sketch a one-dimensional barrier and show why lifetimes are exponentially sensitive to barrier height. (3) Literature reading: from a fission-theory review, summarise two competing asymmetric yield modes [54].

1.11 Problems with solutions

Problem 23.1 — Q from B/A for $A = 238$

Estimate the fission Q-value for a nucleus with $A = 238$ if $(B/A)_{\text{parent}} = 7.6\,\text{MeV}$ and $(B/A)_{\text{fragments}} = 8.5\,\text{MeV}$. Express the result in MeV and comment on its magnitude relative to chemical combustion energies [6, 1].

Solution 23.1

Step 1. From Eq. (1.7),

$$Q = E_B(Y) + E_B(Z) - E_B(X) \approx \left[(B/A)_{\text{frag}} - (B/A)_{\text{parent}}\right] A.$$

Step 2. Substitute the given values:

$$Q \approx (8.5 - 7.6)\,\text{MeV} \times 238 = 0.9 \times 238 = 214\,\text{MeV}.$$

Step 3. Chemical energies are a few eV per reaction. Fission releases $\sim 10^8$ times more energy per event. That is why a few kilograms of fissile material can power a reactor or a weapon [6].

Problem 23.2 — Symmetric SEMF Q algebra

Starting from $M(A, Z)$ in Eq. (1.10) (pairing omitted), derive $Q = -0.26\,a_s A^{2/3} + 0.37\,a_c Z^2/A^{1/3}$ for symmetric fission into two equal fragments. Show that volume and symmetry terms cancel [14, 1].

Solution 23.2

Step 1. $Q = M(A, Z) - 2M(A/2, Z/2)$.
Step 2 (volume). $-a_v A - 2(-a_v A/2) = 0$.
Step 3 (symmetry). Parent: $a_{\text{sym}}(A-2Z)^2/A$. One fragment: $a_{\text{sym}}(A/2-Z)^2/(A/2) = a_{\text{sym}}(A-2Z)^2/(2A)$. Two fragments: $a_{\text{sym}}(A-2Z)^2/A$. Difference vanishes.
Step 4 (surface).

$$a_s A^{2/3} - 2a_s(A/2)^{2/3} = a_s A^{2/3}(1 - 2^{1/3}) = -0.260\,a_s A^{2/3}.$$

Step 5 (Coulomb).

$$a_c\frac{Z^2}{A^{1/3}} - 2a_c\frac{(Z/2)^2}{(A/2)^{1/3}} = a_c\frac{Z^2}{A^{1/3}}(1-2^{-2/3}) = 0.370\,a_c\frac{Z^2}{A^{1/3}}.$$

Step 6. Add surface and Coulomb contributions to obtain Eq. (1.15).

Problem 23.3 — Critical Z^2/A

Using $a_s = 17.8\,\text{MeV}$ and $a_c = 0.711\,\text{MeV}$, evaluate the threshold Z^2/A for $Q > 0$ in symmetric fission. For ^{238}U ($Z = 92$, $A = 238$), is $Q > 0$?

Solution 23.3

Step 1. From Eq. (1.17),

$$\frac{Z^2}{A} > \frac{0.26\,a_s}{0.37\,a_c} = \frac{0.26 \times 17.8}{0.37 \times 0.711} = \frac{4.628}{0.2631} \approx 17.6.$$

Step 2. For ^{238}U,

$$\frac{Z^2}{A} = \frac{92^2}{238} = \frac{8464}{238} \approx 35.6 > 17.6.$$

Yes, $Q > 0$. Uranium is energetically free to fission but is held by the barrier E_f [6, 1].

Problem 23.4 — Barrierless fissility

From the small-deformation result $\Delta E \propto [2a_sA^{2/3} - a_cZ^2/A^{1/3}]$, show that the sphere is unstable when $Z^2/A > 2a_s/a_c$. With $a_s = 17.8\,\text{MeV}$ and $a_c = 0.711\,\text{MeV}$, estimate the critical A if $Z = 0.4A$.

Solution 23.4

Step 1. Instability requires $\Delta E < 0$:

$$2a_sA^{2/3} < a_cZ^2/A^{1/3} \quad \Rightarrow \quad \frac{Z^2}{A} > \frac{2a_s}{a_c}.$$

Step 2.

$$\frac{2a_s}{a_c} = \frac{35.6}{0.711} \approx 50.1.$$

Step 3. With $Z = 0.4A$, $Z^2/A = 0.16A$. Set $0.16A = 50.1 \Rightarrow A \approx 313$. Order-of-magnitude result: nuclei with $A \gtrsim 300$ have no classical liquid-drop barrier in this convention and cannot exist as long-lived species [14, 6].

Problem 23.5 — Photofission competition

At one GDR energy a heavy nucleus has $\sigma_{\text{abs}} = 300\,\text{mb}$ and partial widths $\Gamma_f = 1.5\,\text{MeV}$, $\Gamma_n = 2.0\,\text{MeV}$, and $\Gamma_\gamma = 0.50\,\text{MeV}$. Estimate the photofission cross section. If Γ_n doubles at higher energy while the other quantities remain fixed, what happens? [6, 1]

Solution 23.5

$$b_f = \frac{\Gamma_f}{\Gamma_f + \Gamma_n + \Gamma_\gamma} = \frac{1.5}{4.0} = 0.375, \qquad \sigma_{\gamma f} = \sigma_{\rm abs} b_f = 112.5\,\text{mb}.$$

After Γ_n doubles,

$$b'_f = \frac{1.5}{1.5 + 4.0 + 0.5} = 0.250, \qquad \sigma'_{\gamma f} = 75.0\,\text{mb}.$$

Crossing the barrier does not force fission: neutron evaporation can reduce the fission branch even within a strong absorption region.

Problem 23.6 — Surface vs Coulomb for ε

Using Eqs. (1.26)–(1.28), compute ΔE (in MeV) for ^{238}U at $\varepsilon = 0.1$. Take $a_s = 17.8\,\text{MeV}$, $a_c = 0.711\,\text{MeV}$, $Z = 92$, $A = 238$. Is the sphere stable against this deformation?

Solution 23.6

Step 1.

$$A^{2/3} = 238^{2/3} \approx 38.3, \qquad A^{1/3} \approx 6.20.$$

Step 2.

$$\Delta E = \frac{(0.1)^2}{5}\left[2(17.8)(38.3) - 0.711\frac{8464}{6.20}\right]$$
$$= 0.002(1363 - 971) = 0.002(392) \approx 0.78\,\text{MeV}.$$

Step 3. $\Delta E > 0$: the sphere is stable against this small deformation; a finite barrier remains. (The full barrier height requires a global calculation beyond the quadratic expansion [6, 14].)

Problem 23.7 — Fissility and barrier scales

For ^{238}U, take $Z = 92$, $A = 238$, $a_s = 17.8\,\text{MeV}$, and $a_c = 0.711\,\text{MeV}$. (a) Compute the fissility $x = E_C^{(0)}/(2E_s^{(0)})$. (b) Use the actinide interpolation $E_f(\text{MeV}) \simeq 19.0 - 0.36Z^2/A$. (c) Explain why the positive symmetric-fission Q does not contradict the positive barrier.

Solution 23.7

Step 1: charge-to-mass ratio.

$$\frac{Z^2}{A} = \frac{92^2}{238} = 35.563.$$

Step 2: dimensionless fissility.

$$x = \frac{a_c}{2a_s}\frac{Z^2}{A} = \frac{0.711}{2(17.8)}(35.563) = 0.710.$$

Because $x < 1$, the spherical drop has positive curvature against a small quadrupole deformation; it is not classically barrierless.

Step 3: barrier interpolation.

$$E_f \simeq 19.0 - 0.36(35.563) = 6.20\,\mathrm{MeV}.$$

The numerical agreement with a uranium barrier should not be overinterpreted: the coefficients are an actinide fit and a real actinide has two saddles.

Step 4: energy landscape. The Q-value compares the initial ground state with the final separated fragments, whereas E_f compares the initial state with the highest intermediate deformation. Therefore $Q > 0$ and $E_f > 0$ can hold simultaneously: the final state is lower, but the continuous path first rises.

Bibliography

[1] R. A. Dunlap, *An Introduction to the Physics of Nuclei and Particles* (2nd ed.), IOP Publishing, Bristol (2023), DOI: 10.1088/978-0-7503-6094-4, Ch. 3 (Nuclear composition and size).

[2] W. Demtröder, *Nuclear and Particle Physics*, Undergraduate Lecture Notes in Physics, Springer, Cham (2023).

[3] S. Petrera, *Problems and Solutions in Nuclear and Particle Physics*, UNITEXT for Physics, Springer, Cham (2019).

[4] F. Terranova, *A Modern Primer in Particle and Nuclear Physics*, Oxford University Press (2021).

[5] S. D'Auria, *Introduction to Nuclear and Particle Physics*, Undergraduate Lecture Notes in Physics, Springer, Cham (2018).

[6] K. S. Krane, *Introductory Nuclear Physics*, Wiley, New York (1988).

[7] R. Hofstadter, "Electron scattering and nuclear structure," Rev. Mod. Phys. **28**, 214 (1956).

[8] H. F. Ehrenberg, R. Hofstadter, U. Meyer-Berkhout, D. G. Ravenhall, and S. E. Sobottka, "High-Energy Electron Scattering and the Charge Distribution of Carbon-12 and Oxygen-16," Phys. Rev. **113**, 666 (1959).

[9] H. Yukawa, "On the interaction of elementary particles. I," Proc. Phys.-Math. Soc. Japan **17**, 48 (1935).

[10] R. D. Woods and D. S. Saxon, "Diffuse surface optical model for nucleon-nuclei scattering," Phys. Rev. **95**, 577 (1954).

[11] H. G. J. Moseley, "The high-frequency spectra of the elements," Phil. Mag. **26**, 1024 (1913); **27**, 703 (1914).

[12] C. F. von Weizsäcker, "Zur Theorie der Kernmassen," Z. Phys. **96**, 431 (1935).

[13] P. Cappellaro, *Introduction to Applied Nuclear Physics* (MIT OpenCourseWare / LibreTexts), CC BY-NC-SA 4.0.

[14] J.-L. Basdevant, J. Rich, and M. Spiro, *Fundamentals in Nuclear Physics: From Nuclear Structure to Cosmology*, Springer, New York (2005).

[15] D. Tong, *Particle Physics*, Lecture notes (University of Cambridge / CERN school notes).

[16] M. G. Mayer, "On closed shells in nuclei. II," Phys. Rev. **75**, 1969 (1949).

[17] O. Haxel, J. H. D. Jensen, and H. E. Suess, "On the "magic numbers" in nuclear structure," Phys. Rev. **75**, 1766 (1949).

[18] T. Schmidt, "Über die magnetischen Momente der Atomkerne," Z. Phys. **106**, 358 (1937).

[19] L. W. Nordheim, "On spins, moments, and shells in nuclei," Phys. Rev. **78**, 294 (1950).

[20] Evaluated Nuclear Structure Data File (ENSDF), National Nuclear Data Center, Brookhaven National Laboratory, `https://www.nndc.bnl.gov/ensdf/`.

[21] NuDat 3, National Nuclear Data Center, Brookhaven National Laboratory, `https://www.nndc.bnl.gov/nudat3/`.

[22] N. J. Stone, "Table of nuclear magnetic dipole and electric quadrupole moments," At. Data Nucl. Data Tables **90**, 75 (2005); updated compilations at NNDC.

[23] W. N. Cottingham and D. A. Greenwood, *An Introduction to Nuclear Physics* (2nd ed.), Cambridge University Press, Cambridge (2001).

[24] H. Geiger and J. M. Nuttall, "The ranges of the α particles from the radioactive substances," Phil. Mag. **22**, 613 (1911).

[25] G. Gamow, "Zur Quantentheorie des Atomkernes," Z. Phys. **51**, 204 (1928).

[26] R. W. Gurney and E. U. Condon, "Wave mechanics and radioactive disintegration," Nature **122**, 439 (1928); Phys. Rev. **33**, 127 (1929).

[27] M. Wang, W. J. Huang, F. G. Kondev, G. Audi, and S. Naimi, "The AME 2020 atomic mass evaluation (II). Tables, graphs and references," Chin. Phys. C **45**, 030003 (2021).

[28] Laboratoire National Henri Becquerel (LNHB), Recommended decay data, `http://www.lnhb.fr/nuclear-data/nuclear-data-table/`.

[29] L. M. Langer, R. D. Moffat, and H. C. Price, Jr., "Low energy beta-ray spectra: P^{32} and Cu^{64}," Phys. Rev. **76**, 1725 (1949).

[30] L. M. Langer and H. C. Price, Jr., "Shapes of the beta-spectra of the forbidden transitions of Sb^{124}, Rb^{86}, Sr^{89}, Y^{91}, and Cs^{137}," Phys. Rev. **75**, 1769 (1949).

[31] D. C. Camp and L. M. Langer, "The shape of the ^{66}Ga positron spectrum and the contribution from $0^+ \to 0^+$ transitions," Phys. Rev. **129**, 1782 (1963).

[32] H. C. Verma, *Nuclear Physics: Fundamentals and Applications*, NPTEL/IIT Kanpur lecture series, `https://hcverma.in/ncl_phy_lectures`.

[33] International Atomic Energy Agency, *LiveChart of Nuclides*, evaluated structure, decay, reaction, and fission-yield data, `https://www-nds.iaea.org/relnsd/vcharthtml/VChartHTML.html`.

[34] T. Kibédi, T. W. Burrows, M. B. Trzhaskovskaya, P. M. Davidson, and C. W. Nestor, Jr., "Evaluation of theoretical conversion coefficients using BrIcc," Nucl. Instrum. Methods Phys. Res. A **589**, 202 (2008), DOI: 10.1016/j.nima.2008.02.051.

[35] D. A. Brown *et al.*, "ENDF/B-VIII.0: The 8th major release of the nuclear reaction data library with CIELO-project cross sections, new standards and thermal scattering data," Nucl. Data Sheets **148**, 1 (2018), DOI: 10.1016/j.nds.2018.02.001.

[36] B. Acharya *et al.*, "Solar fusion III: New data and theory for hydrogen-burning stars," Rev. Mod. Phys. **97**, 035002 (2025), DOI: 10.1103/8lm7-gs18.

[37] S. N. Ghoshal, "An experimental verification of the theory of compound nucleus," Phys. Rev. **80**, 939 (1950), DOI: 10.1103/PhysRev.80.939.

[38] D. Adhikari *et al.* (PREX Collaboration), "Accurate determination of the neutron skin thickness of ^{208}Pb through parity-violation in electron scattering," Phys. Rev. Lett. **126**, 172502 (2021), DOI: 10.1103/PhysRevLett.126.172502.

[39] B. T. Reed, F. J. Fattoyev, C. J. Horowitz, and J. Piekarewicz, "Implications of PREX-II on the equation of state of neutron-rich matter," Phys. Rev. Lett. **126**, 172503 (2021), DOI: 10.1103/PhysRevLett.126.172503.

[40] B. Hu *et al.*, "Ab initio predictions link the neutron skin of ^{208}Pb to nuclear forces," Nature Phys. **18**, 1196 (2022), DOI: 10.1038/s41567-022-01715-8.

[41] E. Epelbaum, H.-W. Hammer, and U.-G. Meißner, "Modern theory of nuclear forces," Rev. Mod. Phys. **81**, 1773 (2009), DOI: 10.1103/RevModPhys.81.1773.

[42] H.-W. Hammer, S. König, and U. van Kolck, "Nuclear effective field theory: Status and perspectives," Rev. Mod. Phys. **92**, 025004 (2020), DOI: 10.1103/RevModPhys.92.025004.

[43] T. Otsuka, A. Gade, O. Sorlin, T. Suzuki, and Y. Utsuno, "Evolution of shell structure in exotic nuclei," Rev. Mod. Phys. **92**, 015002 (2020), DOI: 10.1103/RevModPhys.92.015002.

[44] H. Hergert, S. K. Bogner, T. D. Morris, A. Schwenk, and K. Tsukiyama, "The in-medium similarity renormalization group: A novel ab initio method for nuclei," Phys. Rep. **621**, 165 (2016), DOI: 10.1016/j.physrep.2015.12.007.

[45] J. M. Lattimer and M. Prakash, "The equation of state of hot, dense matter and neutron stars," Phys. Rep. **621**, 127 (2016), DOI: 10.1016/j.physrep.2015.12.005.

[46] J. M. Lattimer, "Neutron stars and the nuclear matter equation of state," Annu. Rev. Nucl. Part. Sci. **71**, 433 (2021), DOI: 10.1146/annurev-nucl-102419-124827.

[47] B. P. Abbott *et al.* (LIGO Scientific Collaboration and Virgo Collaboration), "GW170817: Observation of gravitational waves from a binary neutron star inspiral," Phys. Rev. Lett. **119**, 161101 (2017), DOI: 10.1103/PhysRevLett.119.161101.

[48] M. J. Dolinski, A. W. P. Poon, and W. Rodejohann, "Neutrinoless double-beta decay: Status and prospects," Annu. Rev. Nucl. Part. Sci. **69**, 219 (2019), DOI: 10.1146/annurev-nucl-101918-023407.

[49] M. Agostini, G. Benato, J. A. Detwiler, J. Menéndez, and F. Vissani, "Toward the discovery of matter creation with neutrinoless $\beta\beta$ decay," Rev. Mod. Phys. **95**, 025002 (2023), DOI: 10.1103/RevModPhys.95.025002.

[50] P. Gysbers *et al.*, "Discrepancy between experimental and theoretical β-decay rates resolved from first principles," Nature Phys. **15**, 428 (2019), DOI: 10.1038/s41567-019-0450-7.

[51] H. L. Crawford, K. Fossez, S. König, and A. Spyrou, "A vision for the science of rare isotopes," Annu. Rev. Nucl. Part. Sci. **74**, 141 (2024), DOI: 10.1146/annurev-nucl-121423-091501.

[52] Nuclear Science Advisory Committee, *A New Era of Discovery: The 2023 Long Range Plan for Nuclear Science*, U.S. Department of Energy and National Science Foundation (2023), `https://nuclearsciencefuture.org/`.

[53] S. A. Giuliani, Z. Matheson, W. Nazarewicz, E. Olsen, P.-G. Reinhard, J. Sadhukhan, B. Schuetrumpf, N. Schunck, and P. Schwerdtfeger, "Colloquium: Superheavy elements: Oganesson and beyond," Rev. Mod. Phys. **91**, 011001 (2019), DOI: 10.1103/RevModPhys.91.011001.

[54] N. Schunck and D. Regnier, "Theory of nuclear fission," Prog. Part. Nucl. Phys. **125**, 103963 (2022), DOI: 10.1016/j.ppnp.2022.103963.

[55] I. Counts, J. Hur, D. P. L. Aude Craik, H. Jeon, C. Leung, J. C. Berengut, A. Geddes, A. Kawasaki, W. Jhe, and V. Vuletić, "Evidence for nonlinear isotope shift in Yb^+ search for new boson," Phys. Rev. Lett. **125**, 123002 (2020), DOI: 10.1103/PhysRevLett.125.123002.

[56] I. Angeli and K. P. Marinova, "Table of experimental nuclear ground state charge radii: An update," At. Data Nucl. Data Tables **99**, 69 (2013), DOI: 10.1016/j.adt.2011.12.006.

[57] S. Kraemer *et al.*, "Observation of the radiative decay of the ^{229}Th nuclear clock isomer," Nature **617**, 706 (2023), DOI: 10.1038/s41586-023-05894-z.